

# NON-INVASIVE MEASUREMENT OF MOISTURE DISTRIBUTION USING TDR

*Ian Woodhead<sup>1</sup>, Professor Graeme Buchan<sup>2</sup>, Professor Don Kulasiri<sup>3</sup>, Dr Jhon Christie<sup>4</sup>*

<sup>1</sup>Lincoln Technology, Lincoln University, NZ.

<sup>2</sup>Dept Soil and Environmental Physics, Lincoln University, NZ.

<sup>3</sup>Dept. Computing and Biometrics, Lincoln University, NZ.

<sup>4</sup>Streat Instruments Ltd, Christchurch, NZ.

**ABSTRACT.** ‘Time domain reflectometry imaging’ (TDRI) is a new technique for non-invasive measurement of moisture content distribution. A series of TDR measurements taken from one side of the material are inverted using a previously described forward model and iterative improvement of an initial estimated moisture distribution. An adapted conjugate gradient optimisation method that avoids time consuming line searches and employs an electric field surrogate for the Jacobian has provided rapid iteration. Then, coupled with a new blocking technique to accelerate the convergence of buried cells and depending on the initial distribution, between 20 and 100 forward calculations are required to solve a 2-D, 6 by 3 element model.

## 1 INTRODUCTION

Determination of moisture content is of vital interest to a wide range of disciplines and industries. The range of materials is also diverse and includes soil, cereals, dairy products and timber. However, beyond a measure of the mean moisture content, moisture content *profiles* are of interest. Distribution of moisture affects such crucial physical and biological phenomena as drying stresses in timber; moisture and heat transport, solute movement and biological organism behaviour in soil; uniformity of dye absorption in textiles; and the quality of many food products. The capability to characterise moisture gradients or profiles is important for controlling drying processes in materials such as timber and textiles, or to characterise moisture content profiles in soil due to drainage, surface evaporation, plant water uptake or capillarity. Hence a method for non-invasive, non-destructive measurement of moisture profiles would find wide application.

Time domain reflectometry imaging (TDRI) is believed to be a new technique for measurement of moisture distribution. The probing signal comprises the lateral evanescent field of a parallel transmission line (PTL), but could similarly comprise the evanescent field at the end of an open circuited transmission line. A set of TDR measurements for different positions of the PTL relative to the nearby material is inverted to obtain a representation of its permittivity distribution. In our case the permittivity  $\epsilon_r$  is assumed invariant in the axial ( $z$ ) direction, and the PTL is moved in the  $x$ - $y$  plane to resolve  $\epsilon_r$  of cuboid cells with the same length as the PTL (eg 300 mm). Measuring moisture distribution across sawn lumber is an application where this assumption of longitudinal uniformity is reasonable. However, in a block of cheese for example, resolution in the third dimension could be obtained by use of an orthogonal set of measurements. Here, we just describe inversion of 2-D  $\epsilon_r$  data, but when applied to moisture measurement, a dielectric model would be required to translate the resulting  $\epsilon_r$  distribution to moisture content.

Use of the evanescent field as the EM probing signal contrasts with the more conventional microwave imaging, and provides two important advantages. Scattering does not significantly attenuate the signal as occurs with microwave imaging [1], and the use of an evanescent field

provides a spatial resolution that is not inherently limited by the wavelength as in travel time tomography. Diffraction tomography requires both amplitude and phase of the scattered signal to adequately solve the inverse problem [2].

However TDRI requires a very high time measurement resolution ( $< 1$  ps), which determines the depth resolution. Since transverse electromagnetic mode (TEM) propagation is assumed, the width of the PTL must be small compared with the wavelength  $\lambda$ . Hence a practical penetration depth limit is approximately 100 mm with current instrumentation and measurement frequencies.

## 2 METHODS

Fundamental to TDRI is a forward solution to provide a prediction of the pulse propagation time ( $t$ ) on a PTL surrounded by a prescribed, discretised, inhomogenous permittivity distribution. A suitable numerical procedure using a moment method (MM) has been described [3]. We now turn to formulation of the inverse problem, which aims to quantify the  $\epsilon_r$  distribution given a set of propagation velocities representing different positions of the PTL. Although the forward model is currently limited to real  $\epsilon_r$ , it and the inverse solution could be adapted to predict complex values. The inverse solution may be described by:

$$m = g^{-1}(d) \quad (1)$$

where  $m$  is a set of model parameters or values of  $\epsilon_r$ ,  $g$  describes the forward transfer function and includes reliance on other parameters such as PTL geometry and fundamental constants, and  $d$  is a set of observations or readings of  $t$ . Since TDRI forms a non-linear problem, an iterative solution method is required. [4] comment that Quasi-Newton (QN) or conjugate gradient (CG) optimisation is appropriate for this class of problem. The procedure begins with an estimate of the  $\epsilon_r$  distribution  $m_0$ , usually employing *a priori* information. The key parameter in the steepest descent method that also forms the basis for the QN and CG methods, is the weighting factor  $\alpha$  in the recurrence relation:

$$m_{i+1} = m_i - \alpha_i J_i^{-1} \Delta t_i \quad (2)$$

Here the new model  $m_{i+1}$  is derived from the previous permittivity model  $m_i$ , corrected by the weighted product of the sensitivity  $J_i^{-1}$ , and the error in propagation time  $\Delta t_i$ . The magnitude of  $\alpha_i$  controls the step size and its optimal value depends on the local curvature of  $g$ , the accuracy of  $J_i^{-1}$ , and the distance to the solution. As with many optimisation methods, this is ideally determined dynamically, typically using a line minimisation procedure [4].

## 3 THE JACOBIAN

Here, the Jacobian  $J$  has elements  $\frac{\partial t}{\partial \epsilon_r}$  for each cell, and for each position of the PTL, and assumes

linearity around the solution estimate  $m_i$ . A finite difference (FD) method is commonly used to calculate  $J$ , but forms the most computationally intensive step of the inversion, since it requires a forward calculation for each element.

An approximation to  $J$  may be used but if the errors or the step length are large, divergence may result. A method may employ small steps and an inaccurate  $J$  requiring many iterations, or expend additional effort (and hence processing time) to produce an accurate  $J$  to allow larger steps and fewer iterations. The latter method is less likely to diverge due to an inaccurate  $J$ , but calculation of the forward solution and hence  $J$  through FD methods can be very costly in computation time [5]. Consider the following correction  $h_i$  for one iteration of Eqn (2):

$$h_i = \alpha_i [\Delta t_1 \cdots \Delta t_m] \begin{bmatrix} \frac{\partial \varepsilon_{r1}}{\partial t_1} & \frac{\partial \varepsilon_{r2}}{\partial t_1} & \cdots & \frac{\partial \varepsilon_m}{\partial t_1} \\ \vdots & \ddots & & \vdots \\ \frac{\partial \varepsilon_{r1}}{\partial t_m} & \cdots & \cdots & \frac{\partial \varepsilon_m}{\partial t_m} \end{bmatrix} = \alpha_i [\Delta \varepsilon_{r1} \cdots \Delta \varepsilon_m] \quad (3)$$

The correction in  $\varepsilon_{ri}$  comprises the sum of  $\Delta t_i$  for all positions of the PTL, weighted by each corresponding sensitivity. Errors in individual sensitivities lead to incorrect weighting for a cell given a particular set of travel time errors. In the worst case, it may tip the sign of the correction to a cell's  $\varepsilon_{ri}$ , but unless the error is constant and pervasive, the inappropriate correction will increase  $\Delta t_i$ , thereby increasing the cell's weighting and hence the opportunity for the error to be ultimately corrected.

A new linear approximation to  $J$  is now described using a similar concept to that of [6] who derived a Jacobian using electric field strength for geophysical modelling of conductivity. For TDR, [7] showed that the sensitivity of  $t$  to the properties of a small region is a function of the stored energy of the electric field in that region. Extending this idea, it may be shown that for a small contrast in  $\varepsilon_r$ , a surrogate  $J_a$  for the true  $J$  is:

$$J_{a_i} = \left[ k \varepsilon_{ri} |E|_i^2 \right]_{i=1..n} \quad (4)$$

where  $k$  is a constant that may be calculated using an FD approach, and  $E$  is the electric field strength. Accurately determining  $k$  proves unnecessary in this instance, since the line search algorithm dynamically weights  $J$  during inversion.

The use of a 'flatter'  $J_a$  than Eqn 4 provides a greater weight to buried (subsurface) cells that have less influence on  $t$ , and hence converge only slowly. Consequently,  $\varepsilon_r |E|$  was chosen for  $J_a$  rather than  $\varepsilon_r |E|^2$ . Although convergence of buried cells was accelerated, the solution accuracy and the propensity to converge to a particular local minimum was not significantly affected. This supports the contention of [8] that the accuracy of  $J_a$  is not critically important.

While the number of iterations to converge may be quite small, QN and CG methods rely on a line search to locate the minimum for each iteration. Where a FD method is used to construct  $J$ , and the problem is large, this is not a significant drawback, since  $J$  is unchanged during each iteration. Consider for example a modest 10 by 10 2-D inversion. Calculation of  $J$  requires 100 forward calculations, greatly exceeding the number required for even a robust (and hence slow) line search. However for smaller problems more typical of TDRI, or where a rapid  $J_a$  is used, the line search is

a significant overhead. Consequently, an alternative method was used that dynamically alters  $\alpha_i$  to provide a suitable alteration in  $\varepsilon_r$ . During the first iteration but before correcting  $\varepsilon_r$ ,  $\alpha_i$  was altered so the maximum correction in any cell was less than a pre-set threshold, typically  $\varepsilon_r = 3$ . Hence this rapid, straightforward method required no additional forward calculations.

#### 4 EXECUTION

Much of the refinement of the inversion algorithm and the parameter testing used simulated data sets, generated from a model distribution of  $\varepsilon_r$  and the forward solution. The output from the algorithm was a distribution of  $\varepsilon_r$  that ideally matched the initial model.

One characteristic of the MM [3] that greatly speeds up execution of the inverse solution is that the scattering matrix contains mathematical representations of the interactions between the fields in each cell, but is quite independent of the impressed field. Hence the time-consuming effort in calculating the scattering matrix is expended just once for each iteration, and for each PTL position. By contrast, a differential equation (DE) method such as FD, where one forward calculation is required for each PTL position, represents perhaps 20 or 30 forward calculations for each iteration of the inverse solution. Thus while the MM or integral equation (IE) scattering matrices usually take longer to calculate than with DE methods, once applied to an inversion problem, an IE method is much faster. For example the MM method results in a vector of polarisation components  $\mathbf{P}$  described by:

$$\mathbf{P} = \mathbf{K}^{-1} \mathbf{E}_i \quad (5)$$

where  $\mathbf{K}$  is the scattering matrix and  $\mathbf{E}_i$  a vector of impressed field components. Then  $\mathbf{K}^{-1}$  can be calculated for a particular set of model parameters, and matrix multiplication used to determine  $\mathbf{P}$  for each  $\mathbf{E}_i$  defined by a PTL position.

#### 5 THE BLOCKING TECHNIQUE

Despite the improvements in execution speed outlined above, the method usually fails to locate a sufficiently accurate solution. There are several possible reasons for this:

1. The inversion procedure locates and becomes trapped in a local, shallow minimum.
2. The procedure converges to a deep, incorrect minimum yet satisfies the objective function.
3. The correct minimum is located, but even with a small objective function, some parameters are still distant from their target values. In this case the poorly converged parameters (of buried cells) are not sufficiently influential.
4.  $J$  is insufficiently accurate to guide the procedure that consequently dithers around a minimum (despite the observation that convergence was satisfactory with  $J_a = |\mathbf{E}| \varepsilon_r$ , ultimately errors in  $J$  and the forward model lead to dithering).

As convergence proceeds, changes in the model,  $J_i$ , and the distance to the solution influence its optimal value. However they are overshadowed by the change in influence of  $\alpha_i J_i \Delta t_i$  in Eqn (2) due to the shrinking  $\Delta t_i$ . Methods to address this issue have been evaluated to circumvent slow convergence of buried cells, and hence reduce the influence of points 1 to 3 above. Pragmatically, measurement accuracy may render the influence of a buried cell to below the noise floor of the

measuring instrument. Nonetheless, it is advantageous to ensure that the inversion procedure itself does not impose constraints on inversion of measured data.

The principle of blocking is to perturb  $\alpha_i$  so that larger changes are made to the current model during one iteration, and then redistribution of  $\varepsilon_r$  occurs by normal convergence over the next few iterations. Changes to  $\varepsilon_r$  of highly influential cells are blocked during the perturbed iteration, favouring cells with a small influence. The correction during a blocking iteration is determined in the usual manner but uses an alternative  $J_a$  that is exponentially smoothed from several previous  $J_a$ . The perturbation to  $\alpha_i$  is adjusted so that the maximum provisional correction to any non-surface cell is, for example,  $\varepsilon_r = 2$ . In general, the blocking scheme has driven the inversion process into deeper minima than other methods we evaluated.

## 6 RESULTS

The data used for inversion of simulated data comprised 12 measurements of  $t$ , all taken from PTL positions above the material with “unknown”  $\varepsilon_r$ . The distribution of  $\varepsilon_r$  employs the convention that a cell centroid and hence  $\varepsilon_r$  of a cell is represented by a grid-intersection point. The plotting routine used for the figures represent cell values at grid intersections so that the 4 by 3 cell Mprior (the *a priori* distribution) appears as 3 by 2 cells. The chosen target distribution (Table 1) represents dried lumber with a remnant wet centre.

Table 1 and Fig 1 show the solution after 80 iterations, with blocking every eighth iteration. The effect of blocking is to temporarily worsen the objective function, but provide the opportunity to locate minima that are practically beyond the reach of conventional CG inversion.

Table 1. Target (left) and solution from inversion using blocking and a flat *a priori* distribution.

1	1	1	1	1	1	1	1	1	1	1	1
1	1	1	1	1	1	1	1	1	1	1	1
1	1	1	1	1	1	1	1	1	1	1	1
1	5	5	5	5	1	1	5.0	5.0	5.0	5.0	1
1	5	10	10	5	1	1	4.7	12.5	12.5	4.7	1
1	5	5	5	5	1	1	6.3	3.5	3.5	6.3	1

A test of the robustness of a set of inversion parameters is to alter the *a priori* or target distributions, and in this case we have chosen a different target distribution (Table 2) representing the cross-sectional moisture distribution in a block of material that has been non-uniformly dried. This too has resulted in a satisfactory convergence as indicated by the similarity of the solution to the target distribution (Fig 2). The maximum error in propagation time was  $2.8 \times 10^{-14}$  sec.

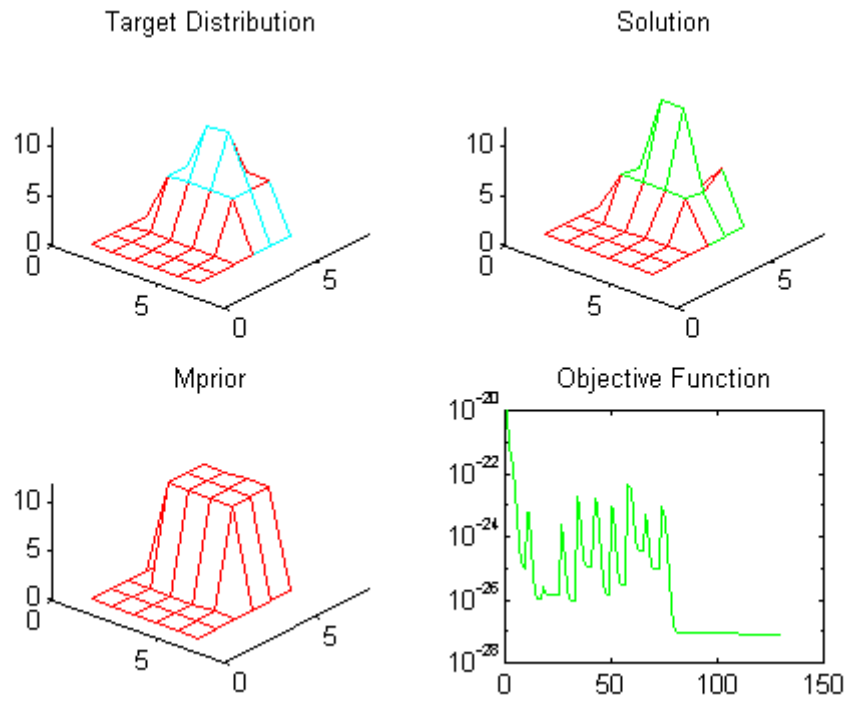


Figure 1. Typical inversion using blocking and a flat *a priori* distribution.

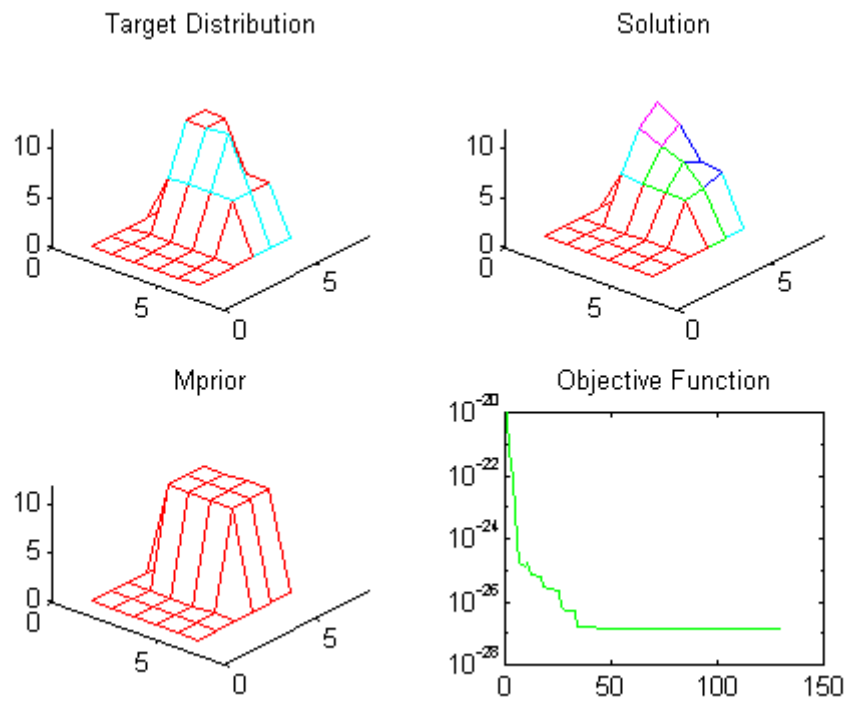


Figure 2. Inversion performance with altered target distribution.

Table 2. Target (left) and solution from inversion with altered target distribution.

1	1	1	1	1	1	1	1	1	1	1	1
1	1	1	1	1	1	1	1	1	1	1	1
1	1	1	1	1	1	1	1	1	1	1	1
1	5	5	5	5	1	1	5.2	5.1	5.1	5.0	1
1	10	10	10	5	1	1	9.1	8.1	7.1	5.4	1
1	10	10	5	5	1	1	10.8	9.3	6.3	5.9	1

## 7 BAYESIAN INVERSION

From the above, it is apparent that acceptable convergence may be obtained from simulated inversion that effectively minimises modelisation errors and assumes perfect instrumentation. Despite the idealised simulation conditions, convergence to a solution that is quite distant from the target or true solution (normally unknown) may occur. In the more realistic situation where a TDR instrument provides a (noisy) set of readings of an unknown distribution, the performance will be further degraded. Hence to reduce the likelihood of the inversion procedure stepping down into an inappropriate minimum, and to accommodate realistic confidence in both the model and the instrumentation, an *a priori* starting distribution needs to be applied. Regularisation may also be required to include additional data to assist convergence to a solution that is close to the target. A reliable *a priori* distribution is critical. In true Bayesian tradition, the *a priori* data is updated or refined by observations, and the weighting applied to each is a measure of the confidence in the measured and *a priori* data sets. The flat starting distributions of Tables 1 and 2 could be considered as null *a priori* data, but more realistic distributions prompt the inversion towards a likely minimum. For example the use of a more “helpful” *a priori* distribution reduced to 20, the required number of iterations in Fig 1, yielding a solution with a maximum error  $\varepsilon_r = 0.8$ .

The above methods have demonstrated rapid convergence with simulated data, but were contingent on a reasonably well-posed set of observations. If necessary, for reasons of noise and/or instrumentation accuracy, additional linearly-independent measurements may be obtained by positioning the PTL on more than one side of the anomalous region, as pointed out by [9]. Measurement uncertainty coupled with errors in forward modelisation, may provide an inconsistent data set to which there is no unique solution, resulting in shallow, poorly defined minima. Other work in progress is mapping the errors to weight individual measurements to minimise these errors.

## 8 CONCLUSIONS

A novel TDRI method has been developed to measure the near-surface moisture distribution in a composite material using CG-based inversion, and evaluated using simulation. A rapidly calculated electric field strength surrogate was used for  $J_a$  and, rather than a computationally intensive line search at each CG iteration, a rapid approximate method was used to determine the CG weighting factor. These refinements significantly reduced the number of forward calculations required for an inversion. To accelerate the convergence of buried and less influential regions of the composite material, a blocking scheme was devised that provided further improvement in inversion performance.

## REFERENCES

- [1] Jofre L, M S Hawley, A Broquetas, E De Los Reyes, M Ferrando, and A Elias-Fuste, Medical Imaging with a Microwave Tomographic Scanner, IEEE Transactions on Biomedical Engineering, vol. 37, pp. 303-311, 1990.
- [2] Johnson S A, D T Borup, J W Wiskin, M J Berggren, M S Zhdanov, K Bunch, and R Eidsens, Report on Collaboration by the Center for Inverse Problems, TechniScan, Inc, Salt lake City, Utah, pp. 1-21, 1996.
- [3] Woodhead I, G Buchan, and D Kulasiri, Modelling TDR Response in Heterogeneous Composite Materials, presented at Third Workshop on Electromagnetic Wave Interaction with Water and Moist Substances, Athens, Georgia, USA, 1999.
- [4] Press W H, S A Teukolsky, W T Vetterling and B P Flannery, *Numerical Recipes in C: The Art of Scientific Computing*, New York, Cambridge University Press, 1997, pp 396-397.
- [5] Ellis R G and D W Oldenburg, Applied geophysical inversion, Geophys. J. Int., pp. 5-11, 1994.
- [6] Farquharson C and D W Oldenburg, Approximate Sensitivities for the Multi-Dimensional Electromagnetic Inverse Problem, presented at International Symposium on Three-Dimensional Electromagnetics, Schlumberger-Doll Research, Ridgefield, Connecticut, 1995.
- [7] Knight J H, Sensitivity of Time Domain Reflectometry Measurements to Lateral Variations in Soil Water Content, Water Resources Research, vol. 28, pp. 2345-2352, 1992.
- [8] Zhdanov M, personal communication, University of Utah, 1999.
- [9] Oldenburg D, personal communication, University of British Columbia, 1999.

Contact point: Ian Woodhead, Lincoln Technology, Lincoln University, Canterbury, New Zealand. Ph: +64-3325-3721; Fax: +64-3325-3725; Email: Woodhead@lincoln.ac.nz.